UltraRapid Communication

Subcortical Ca^{2+} Waves Sneaking Under the Plasma Membrane in Endothelial Cells

Masashi Isshiki, Akiko Mutoh, Toshiro Fujita

Abstract—Subplasmalemmal Ca^{2+}, dynamically equilibrated with extracellular Ca^{2+}, affects numerous signaling molecules, effectors, and events within this restricted space. We demonstrated the presence of a novel Ca^{2+} wave propagating beneath the plasma membrane in response to acute elevation of extracellular [Ca^{2+}], by targeting a Ca^{2+} sensor, cameleon, to the endothelial plasmalemma. These subcortical waves, spatially distinct from classical cytosolic Ca^{2+} waves, originated in localized regions and propagated throughout the subplasmalemma. Translocation of an expressed GFP fused with a PH domain of PLCδ from the plasma membrane to the cytosol accompanied these subcortical waves, and U73122 attenuated not only the GFP-PHδ translocation, but also the peak amplitude of the subcortical Ca^{2+} waves; this finding suggests the involvement of local IP_3 production through PLC-mediated PIP_2 hydrolysis in the initiation of these waves. Changes in NO production as well as PKCβ-GFP translocation from the cytosol to the plasma membrane, but not of GFP-PLA_2 to perinuclear endomembranes, were associated with the subplasmalemmal Ca^{2+} changes. Thus, extracellular Ca^{2+} maintains the basal PLC activity of the plasma membrane, is involved in the initiation of compartmentalized subcortical Ca^{2+} waves, and regulates Ca^{2+}-dependent signaling molecules residing in or translocated to the plasma membrane. The full text of this article is available online at http://circres.ahajournals.org. **(*Circ Res*. 2004;95:e11-e21.)**

Key Words: subplasmalemmal Ca^{2+} ■ FRET ■ cameleon ■ endothelium ■ phospholipase C

Intracellular Ca^{2+} is a second messenger that is spatially and temporally organized for controlling numerous cellular processes. Because of its complex organization consisting of amplitude, frequency, timing, and spatiotemporal patterning, cells display functional specificity and versatility.[1] Ca^{2+} dynamics just beneath the plasma membrane seem to be especially important, because Ca^{2+}-sensitive molecular effectors and cellular processes are compartmentalized in this restricted environment.

Across the plasma membrane, the average intracellular Ca^{2+} concentration ($[Ca^{2+}]_i$) is generally maintained at a level approximately 10 000 times lower than that of extracellular Ca^{2+} ($[Ca^{2+}]_o$) by Ca^{2+} regulators such as Ca^{2+}-ATPase or the Na^+-Ca^{2+} exchanger, which actively regulate the gradients to achieve equilibrium. Although the cytoplasmic surface of the plasma membrane appears to be spatially continuous with the cytosol, it is actually not part of the cytosol and does not have the same [Ca^{2+}] level. It is actually a distinct compartment, differing from other cytosolic regions in terms of the [Ca^{2+}]. The subplasmalemmal Ca^{2+} concentration ($[Ca^{2+}]_{spm}$) in unstimulated cells is ≈10 times higher than the mean cytosolic Ca^{2+} concentration.[2] Changes in $[Ca^{2+}]_{spm}$ are expected to be quite different from those of the overall cytosolic [Ca^{2+}], based on the proximity of Ca^{2+} channels.[3] The heterogeneous structure and biochemical components of the plasma membrane have the potential to create marked differences in Ca^{2+} regulation in the subplasmalemmal space.

Localization of Ca^{2+}-sensitive effector molecules downstream from spatially organized local Ca^{2+} signaling is presumed to be critical for proper cellular functioning. One example is endothelial nitric oxide synthase (eNOS), which is normally localized to the cytoplasmic surfaces of caveolae, specialized microdomains in the plasma membrane, via the acylation process.[4] Mislocalization of eNOS outside the caveolar membrane in nonacylating mutants markedly reduces the sensitivity of the enzyme to Ca^{2+} influx as a trigger for the NO production, a fundamental determinant of cardiovascular homeostasis. In addition to eNOS, some types of adenylyl cyclase localized in cholesterol-rich caveolae, are also sensitive to capacitative Ca^{2+} influx.[5] Not only molecules such as eNOS, which are semifixed to the plasma membrane, but also diffusible cytoplasmic molecules such as PKCβ, which are recruited to the plasma membrane in response to an increase in [Ca^{2+}], would be directly affected by Ca^{2+} influx. However, how those molecules are regulated under basal conditions or in response to the much more localized subplasmalemmal [Ca^{2+}] change is still unclear.

In the last few decades, chelating Ca^{2+} indicators have contributed significantly to research in this field by uncovering information about the spatiotemporal dynamics of cyto-

Original received February 26, 2004; revision received June 24, 2004; accepted June 29, 2004.

From the Department of Nephrology and Endocrinology, Faculty of Medicine, Tokyo University, Tokyo, Japan.

Correspondence to M. Isshiki, Department of Nephrology and Endocrinology, Faculty of Medicine, Tokyo University, Tokyo 113-8655, Japan. E-mail isshiki-tky@umin.ac.jp

Circulation Research **is available at http://www.circresaha.org** **DOI: 10.1161/01.RES.0000138447.81133.98**

solic Ca^{2+} at the single-cell level. Furthermore, the Ca^{2+}-sensitive photoprotein aequorin, with a SNAP-25 targeting motif, has been used for analyzing subplasmalemmal Ca^{2+} in grouped cells.[3] However, the rapid dynamics of subplasmalemmal Ca^{2+} have yet to be visualized with sufficient resolution at the single-cell level, because aequorin is not suitable for imaging because of its weak emission. Recently, however, Miyawaki et al[6] reported on the GFP-based Ca^{2+}-indicating protein, cameleon, one of its advantages being targetability to subcellular locations without loss of imaging at the single-cell level.

To investigate the spatial and temporal aspects of endothelial subplasmalemmal Ca^{2+} dynamics, we used yellow cameleon, which shows intramolecular fluorescence resonance energy transfer (FRET) from ECFP to EYFP in response to Ca^{2+}. Downstream effectors, including eNOS, PKC, and PLA_2, that might also be regulated in response to localized subplasmalemmal Ca^{2+} changes, were likewise examined.

Materials and Methods

Solutions and Chemicals

For experiments that required physiological Ca^{2+}, we used Hank balanced salt solution (HBSS, Invitrogen) containing 1.2 mol/L Ca^{2+}, 1.05 mmol/L $MgCl_2$, and 0.83 mmol/L $MgSO_4$. For experiments that required Ca^{2+}-free conditions, the [$MgCl_2$] of HBSS was adjusted to ≈1.88 mmol/L. 2-Aminoethoxydiphenyl borate (2APB) and ATP was from Sigma Chemical Co. Ionomycin was from Calbiochem.

Vectors and Transfection

The motif used to target YC to the plasma membrane was the 20-amino acid-long, doubly palmitoylated[7,8] amino terminal portion of neuromodulin (also called as GAP43). This motif is known to target GFP mutants to the plasma membrane[2,9] and the chimeric protein of YC with the membrane-targeting motif at its N-terminus was designated NYC. NYC was generated as described previously[2] from native YC2.1 (kindly provided by Drs R. Tsien, Howard Hughes Medical Institute, UCSD, La Jolla, Calif, and A. Miyawaki, RIKEN Wako Institutes, Saitama, Japan). The mitochondrial targeting sequence (MTS) was amplified by PCR using a pECFP-Mit vector (Clontech) as a template and the PCR product with *Hin*dIII sites at both ends was subcloned into the *Hin*dIII sites of YC2.1-pcDNA3, which is 18 nucleotides upstream from the initiation codon of YC2.1. The expression vectors for CFPmem, YFPmem, and PKCβ-GFP were purchased from Clontech. The vectors for PLCδ1PH-GFP[10] and GFP-PLA_2 were kindly provided by Drs T. Balla (National Institute of Child Health and Development, Bethesda, Md) and T. Hirabayashi (Chiba University, Chiba, Japan), respectively. Subconfluent endothelial cells were transiently transfected with the indicated cDNA using lipofectamine 2000 (Invitrogen Corp). One day after transfection, the cells were transferred to 35-mm glass-bottom culture dishes (Mat Tex Corp).

DAF-2 Loading

For NO measurement, loading of DAF-2 (Daiichi Pure Chemicals Co, Ltd) into the cell was performed as previously described.[2]

Imaging

All of the images were obtained with a Leica confocal microscopy system (Leica) equipped with an argon laser, inverted microscope, galvano stage, and oil immersion objectives of ×100 and ×40 (PL APO, Leica) with NA values of 1.4 and 1.25, respectively.

Images in Figures 1 and 4 were obtained with a ×100 objective, and their lateral and axial resolutions are theoretically 0.17 and 0.82 μm, respectively, under optimal optical conditions.[11,12] The pixel size of such images is 0.24 μm/pixel, and the *z*-distance between image planes in Figure 1B is ≈1.5 μm. *x-z* images were obtained using the galvano stage. Other images were obtained with a ×40 objective, and their lateral and axial resolutions are 0.20 and 1.03 μm, respectively. Pixel size ranges from 0.37 to 0.73 μm depending on the magnification for each image.

Cells transfected with Ca^{2+} indicating sensors (YC, NYC, and mitYC) were excited at 514 nm and an emission wavelength of 530 to 550 nm was acquired for subcellular localization of the sensors. For the analysis of FRET, cells expressing the sensors were excited at 456 nm and image pairs of donor CFP (480±10 nm) and acceptor YFP (515±10 nm) were acquired simultaneously. We designated the 505 to 525 nm/470 to 490 nm (acceptor/donor) emission ratio, which is a measure of bound Ca^{2+}, as the FRET image. To capture the propagation of subplasmalemmal Ca^{2+} waves, images of 128×128 pixels were obtained at the fastest interval of 0.14 seconds by the reciprocal mode of 1000-Hz line scanning.

Cells loaded with DAF-2 or expressing GFP chimeras, including PKCβ-GFP and GFP-PLA_2, were excited at 488 nm, and a 500- to 540-nm emission was acquired.

Regions of interest (ROI) were traced on the monitor and the ratio value of YFP/CFP for each ROI was calculated using a built-in accessory program in the confocal system. The processing of ratio images was done off-line using the ratio imaging module of OpenLab software (Improvision Inc). Recordings of subplasmalemmal Ca^{2+} waves were made in more than 30 cells, and experiments other than DAF-2 monitoring were performed in ≈10 cells. NO recording in DAF-2–loaded cells was performed ≈20 times in grouped cells (≈200 cells). All of the data presented are representative of multiple experiments yielding similar results.

Results

The chimeric YC protein with the membrane-targeting motif at its N-terminus was generated as described in Materials and Methods (Figure 1A, NYC). Endothelial cells were transiently transfected with YC or NYC. NYC was uniformly distributed on the cell surface, whereas native YC was expressed predominantly in the cytosol as revealed by thin-slice *x-y* confocal images (Figure 1B and 1C). An *x-z* image of cells expressing NYC revealed the dome-like distribution of this chimeric protein above the cell body, which was ≈10 μm in height and often had thin edges or lamellipodia (Figure 1C, red arrow). In intact cells, attachment of the 20 amino acid–long tag to the N-terminus of YC did not affect the Ca^{2+}-dependent increase in the emission ratio, which reflects FRET efficiency.[2]

First, we examined how the extracellular Ca^{2+} concentration ($[Ca^{2+}]_o$) might affect the subplasmalemmal Ca^{2+} concentration ($[Ca^{2+}]_{spm}$), by exposing NYC-expressing cells sequentially to medium containing nominally no Ca^{2+}, 0.1 mmol/L EGTA, and then 1.2 mmol/L Ca^{2+}. In nominally Ca^{2+}-free medium, the ratio images revealed heterogeneous values for the ratio within single cells. For example, the subcellular region at a portion near the edges showed a somewhat higher emission ratio than other regions (Figure 2A, 0.57 seconds; Figure 2B, 0.88 in R1 and 0.84 in R2 and R3). The difference was estimated to be ≈150 nmol/L based on our previously reported calibrating method.[2] Images collected at 0.14-second intervals showed the differential sensitivity of the plasma membrane to changes in the $[Ca^{2+}]_o$. Acute depletion of extracellular Ca^{2+} with 0.1 mmol/L EGTA decreased the $[Ca^{2+}]_{spm}$ within a second, but with a slight lag of 1 frame (0.14 seconds) in the R3 region, which appeared to represent the lamellipodium (Figure 2A, 1.29, 1.43 seconds).

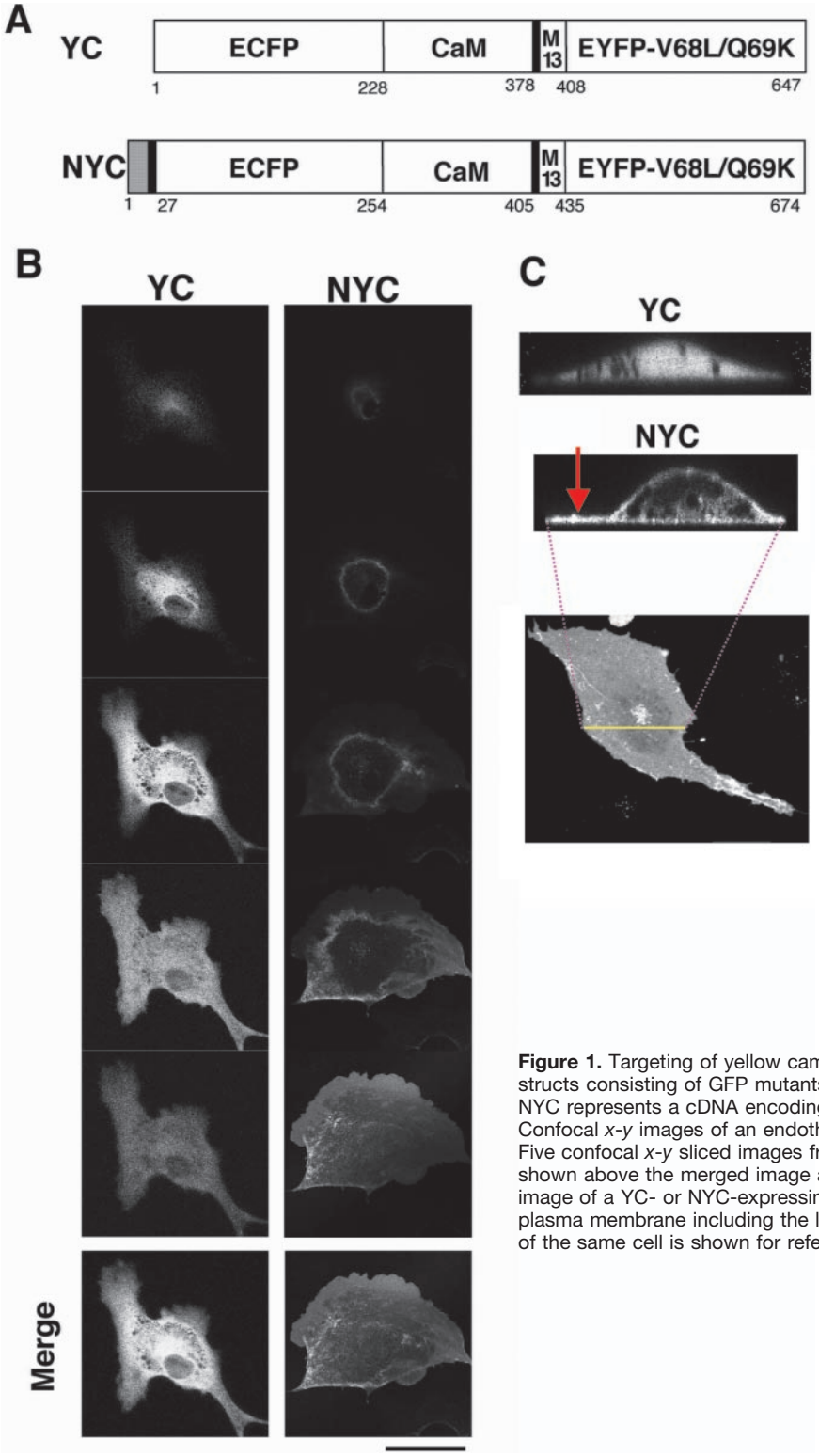

Figure 1. Targeting of yellow cameleon to the plasma membrane. A, Constructs consisting of GFP mutants (YC, NYC). Shaded box at the 5′ end of NYC represents a cDNA encoding the 20 amino acids of neuromodulin. B, Confocal *x-y* images of an endothelial cell transiently expressing YC or NYC. Five confocal *x-y* sliced images from the apex to the base of the cell are shown above the merged image at the bottom (Bar=20 μm). C, Confocal *x-z* image of a YC- or NYC-expressing cell. NYC is correctly targeted to the plasma membrane including the lamellipodium (red arrow), and an *x-y* image of the same cell is shown for reference.

Most strikingly, repletion with 1.2 mmol/L Ca^{2+} initiated a simultaneous increase in $[Ca^{2+}]_{spm}$ in R1 and R2 (pink arrows at 13.30 seconds in Figure 2A), which then propagated throughout the plasma membrane in the form of Ca^{2+} waves (Figure 2A, 13.30 to 14.87 seconds). The two Ca^{2+} waves originating from such regions fused and finally propagated to R3, representing the lamellipodium. The movie file of this experiment can be found in the online data supplement at http://circres.ahajournals.org. There is usually a single initiation site in a cell, but 3 of the 11 cells examined had multiple sites: two with two hot spots and one with three. Based on our observation of multiple cells, the velocity of Ca^{2+} wave propagation was determined to be (mean±SD) 56±26 μm/s (range, 24 to 105 μm/s). Throughout the recording of traces

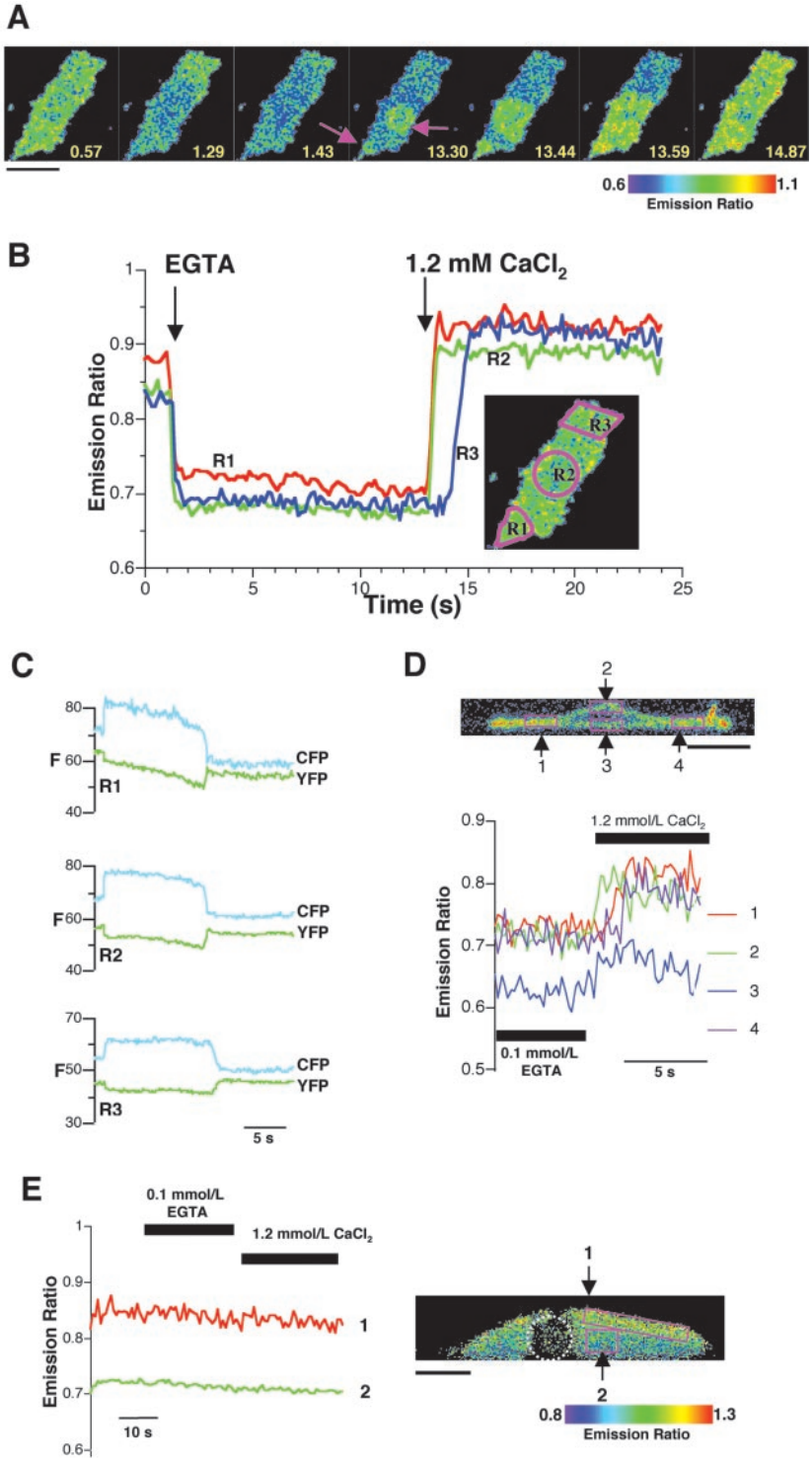

Figure 2. Spatio-temporal imaging of subplasmalemmal Ca^{2+}. A, Cell expressing NYC was excited at 456 nm and image pairs of donor CFP (480±10 nm) and acceptor YFP (515±10 nm) were collected 0.14 seconds apart. Ratio images of YFP/CFP are shown. Time at the lower right-hand corner of each ratio image corresponds to the time-point of the trace shown in B. Increasing $[Ca^{2+}]_o$ causes the appearance of subcortical Ca^{2+} waves originating from small localized regions (indicated with pink arrows at 13.3 seconds) propagating throughout the cell (Bar=50 μm). B, Time-course of subcellular $[Ca^{2+}]_{spm}$ changes in the NYC-expressing cell. Three distinct subcellular regions are designated R1, R2, and R3, as indicated in the inset. In response to the indicated addition of 0.1 mmol/L EGTA and 1.2 mmol/L $CaCl_2$, the $[Ca^{2+}]_{spm}$ in each of the three regions (R1 in red, R2 in green, and R3 in blue) decreased, and then increased again with different kinetics. C, Time-course of changes in the fluorescence intensity (F, arbitrary unit) of CFP and YFP in each of the three regions in R1–3 in B. D, Difference in kinetics of $[Ca^{2+}]_{spm}$ between the apical and basal aspects of NYC-expressing cells. Time-courses of changes in the emission ratios for 4 different subcellular regions, (1 through 4), as indicated in the false-colored ratio *x-z* image, are shown (Bar=20 μm). In response to an increase in $[Ca^{2+}]_o$, $[Ca^{2+}]_{spm}$ in the apical aspect of the cell (2, green line) begins to increase first, whereas the increase in the basal aspect (3, blue line) is slower and the peak $[Ca^{2+}]_{spm}$ in the basal aspect is lower than that in the apical membrane (1, 2, and 4). E, Time-courses of changes in the emission ratios for two cytosolic regions near (1, red) and apart from (2, green) the apical plasma membrane in *x-z* images of a YC-expressing cell. Initial false-colored ratio image with indicated ROIs is shown on the right. Dotted circle in the cell indicates the nucleus (Bar=10 μm).

of the emission intensity of ECFP and EYFP at R1, R2, and R3, mirror images were created to ensure that the ratio changes reflected real changes in FRET from donor ECFP to acceptor EYFP (Figure 2C). Furthermore, because DsRed can be used as a FRET partner with GFP,[13] we changed the donor and acceptor pairs in the sensor molecule NYC from ECFP/EYFP to EGFP/DsRed. We also confirmed correct membrane targeting of the new sensor, which detected similar $[Ca^{2+}]_o$-dependent FRET changes and subplasmalemmal waves (data not shown). Such FRET changes were, however, not observable in cells doubly transfected with ECFPmem and EYFPmem, control molecules of ECFP and EYFP, respectively. Each has the same membrane-targeting motif at the N-terminus as NYC (data not shown). Thus, we can rule out artifacts possibly caused by pH-dependent changes in YFP fluorescence.[14] Interestingly, $[Ca^{2+}]_{spm}$ are similar at the apical aspect of the cell body and at the lamellipodium, whereas $[Ca^{2+}]_{spm}$ at the basal aspect of the cell body is lower

and changes more gradually than in other regions during experimental manipulation of $[Ca^{2+}]_o$ (Figure 2D). Thus, the subplasmalemmal Ca^{2+} waves with sharp wavefronts presumably propagate preferentially to the apical side of the subplasmalemma, where $[Ca^{2+}]_o$ changes can be directly and rapidly affected. An *x-z* image of a YC-expressing cell revealed the existence of a subplasmalemmal region beneath the apical side of the plasma membrane with a somewhat higher $[Ca^{2+}]$ (Figure 2E). However, $[Ca^{2+}]_o$ changes hardly affected $[Ca^{2+}]$ in any cytosolic regions in YC-expressing cells (Figure 2E), suggesting the Ca^{2+} wave detected by NYC propagates through a restricted subplasmalemmal space with less vertical thickness than the optical resolution of our experimental system.

Cells expressing YC in bulk cytosol can detect only small, if any, increases in the emission ratio in response to an acute increase in $[Ca^{2+}]_o$ from 0 to 1.2 mmol/L (Figure 3A). This is in contrast to the dramatic ratio increase detected by NYC (Figure 2B). Although the minimum (R_{min}) and maximum ratio value (R_{max}) are required for calibration in each experiment, R_{min} in YC- or NYC-expressing cells is usually very close to the ratio obtained when the cells are in Ca^{2+}-free extracellular condition with EGTA.[2] Thus, if we assume the minimum and maximum ratio values in Figure 3A to be 1.08 and 1.7, respectively, the percent emission ratio increase (ERI) in YC-expressing cells in response to 1.2 mmol/L $CaCl_2$ is only 6%. In contrast, NYC-expressing cells usually experience more than 50% ERI, as calculated with R_{max} obtained by adding 10 μmol/L ionomycin+10 mmol/L $CaCl_2$ (data not shown). Thus, bulk cytosolic YC compromises the resolution of NYC-detectable subplasmalemmal Ca^{2+} waves because the proportion of the subplasmalemmal volume is small and such a localized signal becomes less clear because of the background fluorescence of a much larger fraction of nonsubplasmalemmal cytosol. Interestingly, NYC cannot detect the YC-detectable global $[Ca^{2+}]$ transient induced by ATP under nominally Ca^{2+} free conditions (Figure 3B). This suggests a steep Ca^{2+} gradient of global waves, with lower $[Ca^{2+}]$ at the outer rim of the wavefront not exceeding $[Ca^{2+}]_{spm}$. 2-APB, a putative modulator of the IP_3 receptor,[15] the Ca^{2+}-release activated Ca^{2+} channel,[16] or some of the transient receptor potential (TRP) superfamily,[17] dose-dependently decreased the basal level of $[Ca^{2+}]_{spm}$ (Figure 3C) with little effect on bulk cytosolic $[Ca^{2+}]$ (data not shown), suggesting the involvement of 2-APB–sensitive mechanisms in the maintenance of the steep $[Ca^{2+}]$ gradient between the subplasmalemma and the bulk cytosol.

To confirm that the Ca^{2+} waves detected only with NYC are confined to the subplasmalemmal space, we examined whether treatment with 1.2 mmol/L $CaCl_2$ also affected the intramitochondrial Ca^{2+} concentration using mit-YC, a mitochondria-targeting version of YC (Figure 4A). Expression of mit-YC was found by confocal microscopy to be localized to the thin tubes, typical architectural features of mitochondria. Close examination of serial *x-z* images of a mit-YC–expressing cell revealed a number of dots, which are cross sections of such tubes (Figure 4B). Some of the dots, distributed within the cell, were very close to but apparently not touching the plasma membrane. In nominally Ca^{2+}-free

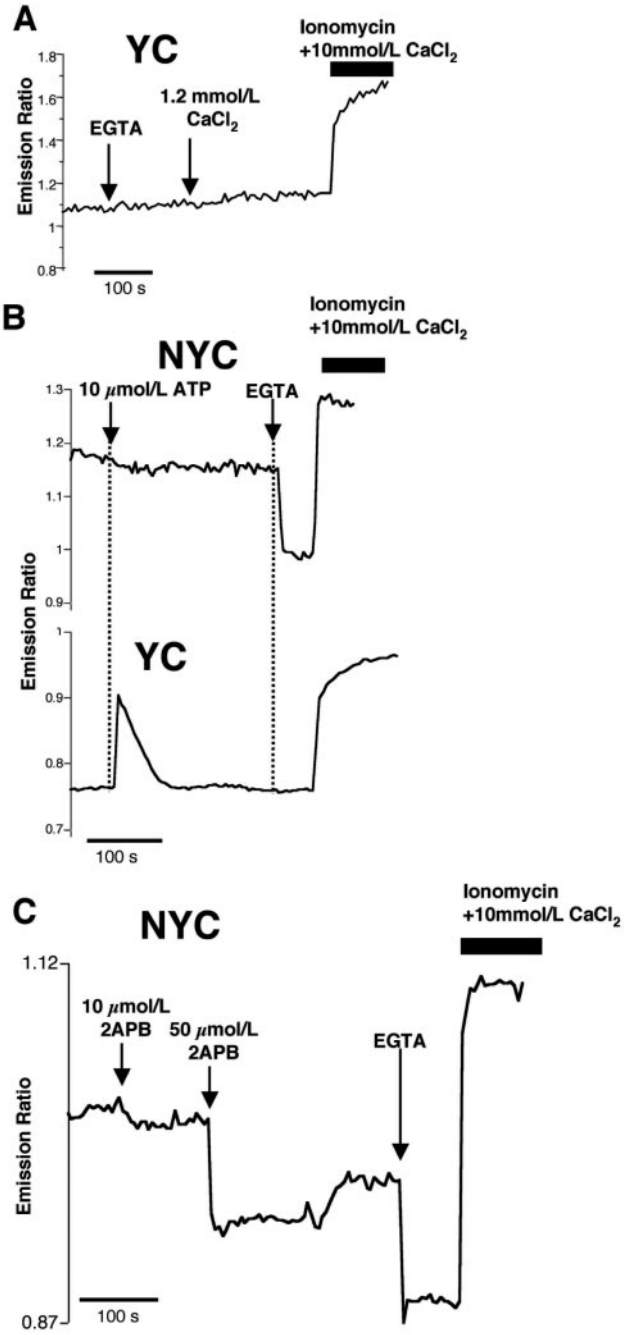

Figure 3. YC and NYC detect distinctly compartmentalized Ca^{2+}. A, Cell expressing YC in nominally Ca^{2+}-free medium was sequentially exposed to 0.1 mmol/L EGTA, 1.2 mmol/L $CaCl_2$, and then 10 μmol/L ionomycin+10 mmol/L $CaCl_2$ (thick bar). B, Cell expressing either NYC or YC was stimulated with 10 μmol/L ATP in medium nominally free of extracellular Ca^{2+}, and then sequentially exposed to 0.1 mmol/L EGTA, and 10 μmol/L ionomycin+10 mmol/L $CaCl_2$, as indicated. C, 2-APB decreased the basal level of $[Ca^{2+}]_{spm}$ detected by NYC.

medium, 10 μmol/L ATP evoked an intramitochondrial Ca^{2+} transient (Figure 4C), similar in shape to that detected by YC (Figure 3B, bottom), suggesting that subdomains with high cytoplasmic $[Ca^{2+}]$ are associated with a $[Ca^{2+}]$ rise in the neighboring mitochondria and that the signal detected by mit-YC is another reflection of $[Ca^{2+}]$ in a portion of the cytosol not including the subplasmalemma. Rapid exchange

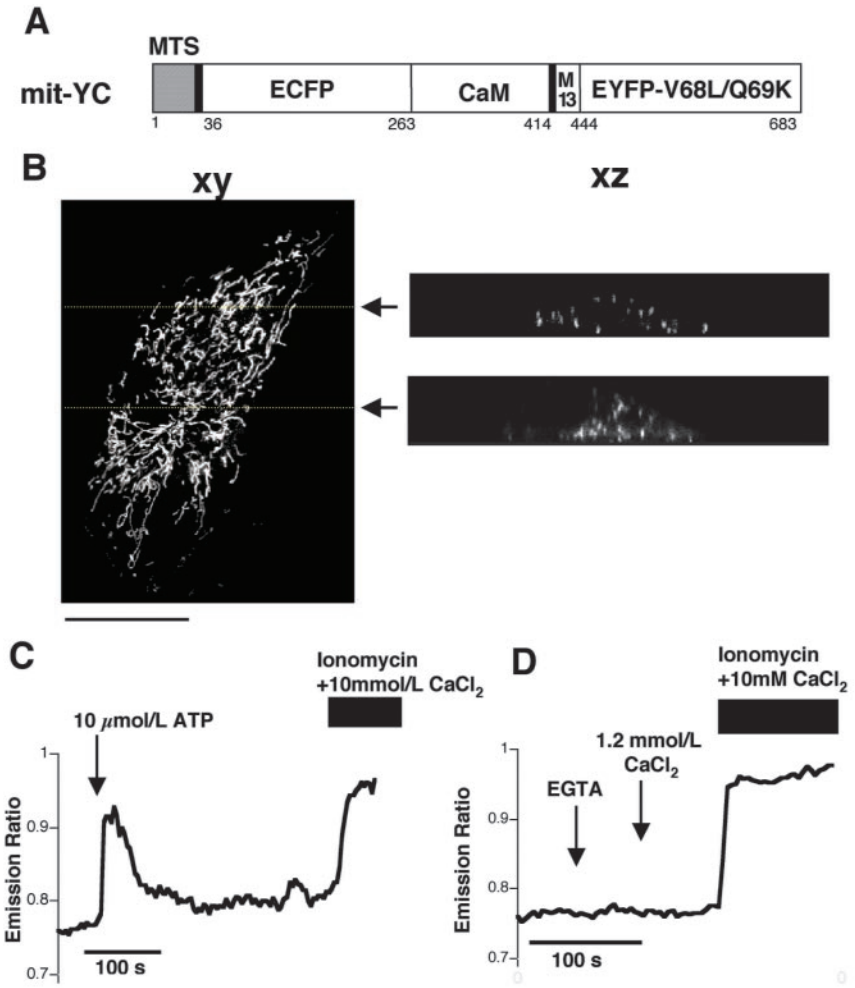

Figure 4. Yellow cameleon (YC) targeted to mitochondria detects $[Ca^{2+}]$ associated with portion of cytosol not including subplasmalemma. A, Constructs consisting of mitochondria-targetable YC (mit-YC). Shaded box at the 5′ end of mit-YC represents a cDNA encoding a mitochondrial targeting sequence (MTS) derived from the precursor of subunit VIII of human cytochrome C oxidase. B, Confocal *x-y* and *x-z* images of an endothelial cell transiently expressing mit-YC (excitation wavelength 514 nm, emission wavelength 530 to 550 nm, Bar=20 μm) C, ATP-induced Ca^{2+} transient detected by mit-YC. D, Acute change in $[Ca^{2+}]_o$ does not affect intramitochondrial $[Ca^{2+}]$.

of Ca^{2+} free extracellular medium to 1.2 mmol/L–containing medium did not affect $[Ca^{2+}]$ detected by mit-YC (Figure 4D), suggesting that the subplasmalemmal Ca^{2+} wave detected by NYC propagates through a very confined space beneath the plasma membrane not reaching the mit-YC–detectable subdomains.

Next, to examine whether phosphatidylinositol 1,4,5-trisphosphate (IP_3) plays a role in the origin of subcortical Ca^{2+} waves, we monitored spatiotemporal changes in the plasmalemmal phosphatidylinositol 4,5-bisphosphate (PIP_2) pool and its hydrolyzed product, IP_3. The PLCδ pleckstrin homology (PH) domain-GFP fusion protein expressed in a cell was exposed to treatments inducing the propagation of subcortical Ca^{2+} waves. PLCδPH is known to specifically bind with PIP_2 or IP_3, and to be rapidly redistributed from the plasma membrane to the cytosol in response to PLC activation by receptor stimulation, or by an increase in Ca^{2+} itself.[10] Translocation of PLCδPH-GFP also reflects an increase in the cytoplasmic IP_3 concentration ($[IP_3]_i$), and Ca^{2+}-mediated enhancement and suppression of $[IP_3]_i$ have been proposed to be involved in organizing complex Ca^{2+} signaling patterns.[18] As in other cell types, most of the PLCδPH-GFP fluorescence expressed in the endothelium was confined to the plasma membrane in the Ca^{2+}-free medium (Figure 5A). An acute increase in $[Ca^{2+}]_o$ from 0 to 1.2 mmol/L caused translocation of PLCδPH-GFP from the plasma membrane to the cytosol, indicative of PIP_2 hydrolysis and IP_3 production through PLC activation, which was ≈20% of the maximum translocation produced by 10 μmol/L ATP (Figure 5B and 5C). An increase in $[Ca^{2+}]_{spm}$ can mediate PIP_2 hydrolysis through PLC activation because PLC activity is dependent on Ca^{2+}.[19] The opposite could also occur if locally produced IP_3 causes local Ca^{2+} influx, as discussed later. In fact, U73122, an inhibitor of PLC, attenuated the rate of increase and the peak value of the $[Ca^{2+}]_o$-dependent $[Ca^{2+}]_{spm}$ increase (Figure 5D), as well as translocation of PLCδ-GFP from the plasma membrane to the cytosol (Figure 5C). Accordingly, PLC hydrolysis may be at least partially associated with the positive feedback system of subcortical Ca^{2+} wave formation.

We then examined how such a locally organized Ca^{2+} increase exerts specificity of downstream signaling. PKC and PLA_2, both of which are Ca^{2+}-sensitive signaling molecules, are known to be localized in the cytosol in the unstimulated state. Through the common C2 domain, PKC and PLA_2 are translocated to different membrane domains, the plasma membrane, and the perinuclear endomembranes, respectively. Translocation of these molecules in response to treatment that can evoke subcortical Ca^{2+} waves was monitored by fusing GFP to each molecule. When transiently expressed in endothelial cells, PKCβ-GFP was found in the cytosol (Figure

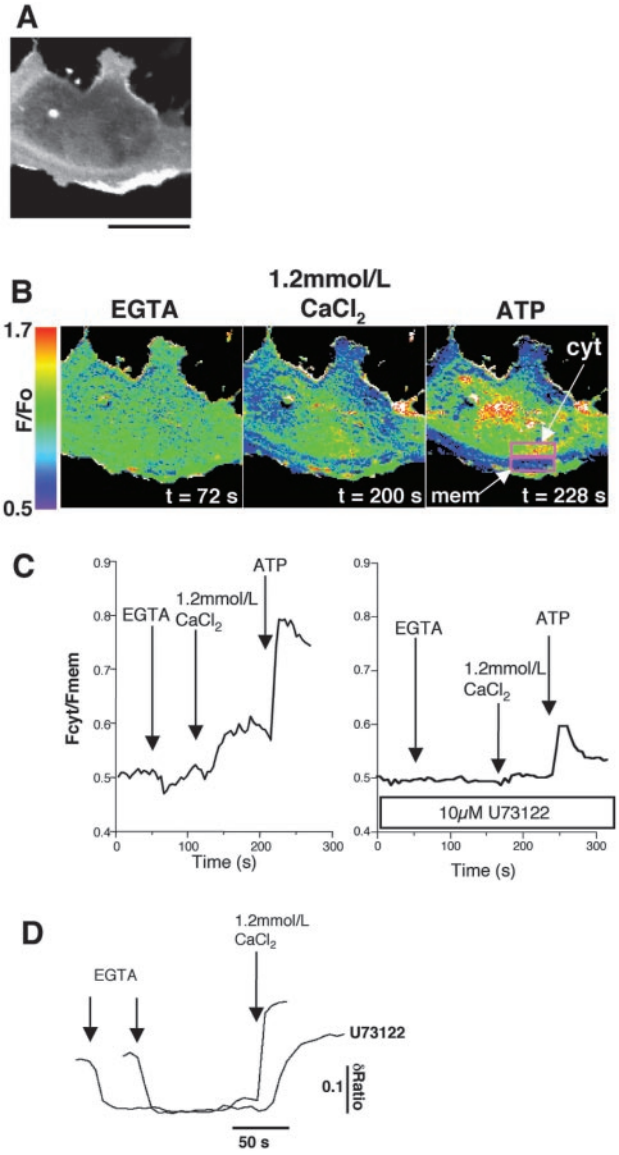

Figure 5. PIP_2 hydrolysis contributing to the organization of subcortical Ca^{2+} waves in response to extracellular Ca^{2+} levels. A, Confocal image of an endothelial cell in nominally Ca^{2+}-free medium transiently expressing PLCδPH-GFP (Bar=20 μm). B, False-color ratio images were generated by dividing each image by the initial image at t=0 seconds. Cell was sequentially exposed to 0.1 mmol/L EGTA, 1.2 mmol/L $CaCl_2$, and 10 μmol/L ATP. Time shown at the lower right-hand corner of each image corresponds to the time-point of the trace shown on the left of C. Translocation of PLCδPH-GFP was monitored by the cytosol (cyt) to plasma membrane (mem) fluorescence ratio shown in the rectangular areas in the right-hand image in B. C, EGTA (0.1 mmol/L), 1.2 mmol/L Ca^{2+}, and then 10 μmol/L ATP were added to the nominally Ca^{2+}-free medium as indicated, with or without 10 μmol/L U73122. D, Effect of 10 μmol/L U73122 (10 μmol/L) on the subplasmalemmal Ca^{2+} wave.

6A). Stimulation-induced translocation of PKCβ, one of several Ca^{2+}-sensitive PKC subtypes, was evaluated by the plasma membrane to cytosol fluorescence ratio. In contrast to the rapid and dramatic translocation of PKCβ-GFP from the cytosol to the plasma membrane induced by ATP or ionomycin, both of which can elevate cytosolic $[Ca^{2+}]_i$, an acute increase in $[Ca^{2+}]_o$ from 0 to 1.2 mmol/L transiently induced 5% to 10% of the maximum translocation induced by ATP in the presence of a physiological level of $[Ca^{2+}]_o$ (Figure 6B and 6C). Similar to PKCβ-GFP, GFP-PLA_2 also appeared to be homogeneously expressed in the cytosol in unstimulated endothelial cells (Figure 7A). Stimulation-induced translocation of PLA_2 was evaluated by the perinuclear endomembrane to whole cell fluorescence ratio. When stimulated with ATP and thapsigargin under conditions nominally free of extracellular Ca^{2+}, intended to mobilize intracellular Ca^{2+} from intracellular ER Ca^{2+} stores, an acute but transient accumulation of fluorescence in the perinuclear endomembranes was observed (Figure 7B, t=64 seconds, arrow, Figure 7C). After restoration to the basal level, the addition of 1.2 mmol/L extracellular Ca^{2+}, which can induce capacitative Ca^{2+} entry, fluorescence again accumulated in the same perinuclear endomembranes, but with slower kinetics and a lower peak intensity (Figure 7B, t=354 seconds, Figure 7C). A final addition of ionomycin induced rapid and more intense fluorescence accumulation (Figure 7B, t=435 seconds, Figure 7C). In contrast to this translocation that is sensitive to bulk cytosolic Ca^{2+}, however, acute elevation of $[Ca^{2+}]_o$, which can increase $[Ca^{2+}]_{spm}$, did not induce GFP-PLA_2 accumulation in perinuclear endomembranes (Figure 7D). This is in marked contrast to the partial translocation of PKCβ-GFP in response to an increase in $[Ca^{2+}]_{spm}$.

Lastly, we examined how the activity of eNOS, a Ca^{2+}-sensitive molecule localized to the inner surfaces of endothelial membrane microdomains, may be affected by $[Ca^{2+}]_o$. Endothelial cells loaded with the NO indicator DAF-2 were sequentially exposed to nominally Ca^{2+}-free medium, 0.1 mmol/L EGTA, 1.2 mmol/L Ca^{2+}, and then 10 mmol/L Ca^{2+}+10 μmol/L ionomycin (Figure 8). In response to the acute increase in $[Ca^{2+}]_o$, DAF-2 fluorescence gradually increased, which was abolished by L-NAME, indicating that $[Ca^{2+}]_o$-dependent increases in $[Ca^{2+}]_{spm}$ can affect eNOS activity. Although the relative DAF-2 fluorescence increase induced by this $[Ca^{2+}]_o$ manipulation was less than 30% of the maximum activation by 10 μmol/L ionomycin+10 mmol/L Ca^{2+}, NO production is clearly sensitive to $[Ca^{2+}]_o$.

Discussion

The subplasmalemmal spatiotemporal aspects of Ca^{2+} dynamics sensitive to $[Ca^{2+}]_o$ were examined using cameleon and a FRET-based technique. Our observations appear to be consistent with those of a previous study using aequorin, in which a dramatic increase in $[Ca^{2+}]_{spm}$ in A7r5 cells was detectable only when the sensor was expressed on the cytoplasmic face of the plasma membrane.[3] Cameleon is superior to aequorin in terms of its imaging feasibility based on the intense fluorescence emitted from GFP mutants; consequently, subplasmalemmal Ca^{2+} waves were observed and characterized for the first time in this study. These subcortical Ca^{2+} waves cannot be detected by conventional imaging methods using indicators such as Indo-1, Fluo-4, or native YC that are nonspecifically loaded or expressed in the cytosol. Bulk cytosolic Ca^{2+} waves, which have been well described, basically consist of Ca^{2+} released from internal stores. Unlike the bulk cytosolic Ca^{2+} waves, the Ca^{2+} source for subplasmalemmal waves is extracellular Ca^{2+}, and these

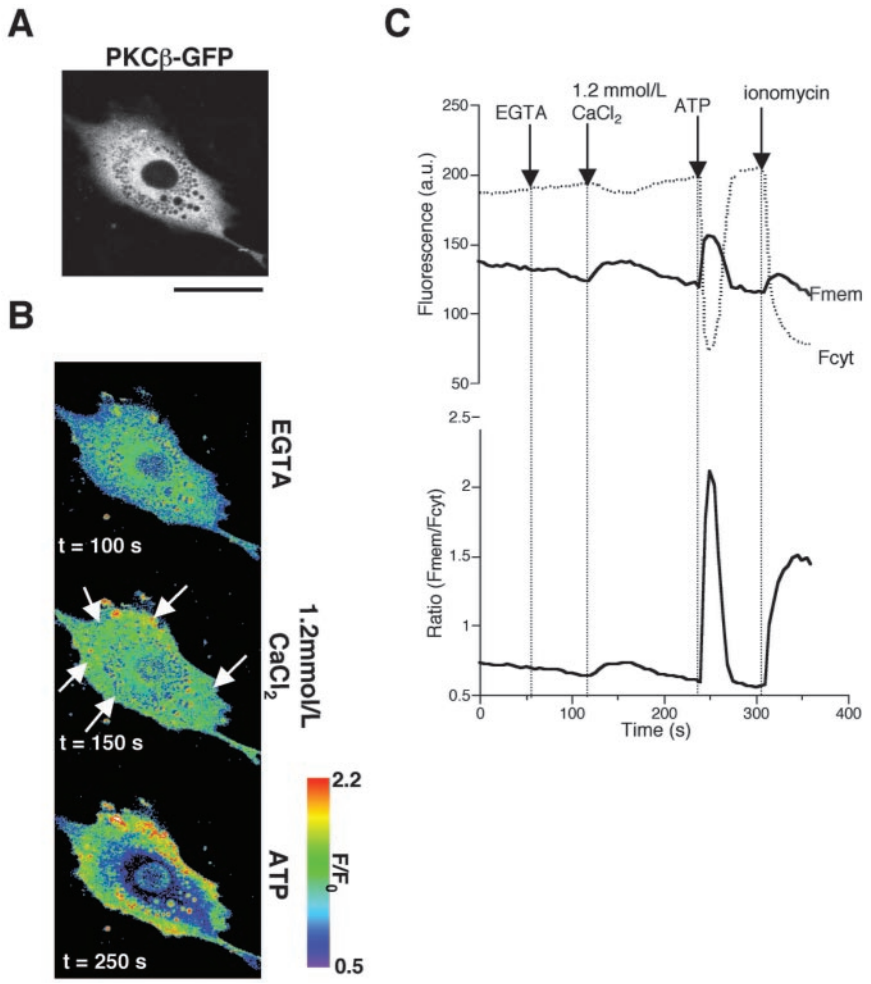

Figure 6. PKCβ-GFP translocation from cytosol to the plasma membrane occurs in association with an acute increase in $[Ca^{2+}]_{spm}$. A, Confocal cell image in nominally Ca^{2+}-free medium transiently expressing PKCβ-GFP (Bar=20 μm). B, False-color ratio images were generated by dividing by the initial image at t=0 seconds shown in A. Cell was sequentially exposed to 0.1 mmol/L EGTA, 1.2 mmol/L $CaCl_2$, and 50 μmol/L ATP. Time shown at the lower left-hand corner of each image corresponds to the time-point of the trace shown in C. Increase in $[Ca^{2+}]_o$ from 0 to 1.2 mmol/L induced an increase in fluorescence at the cell edges (1.2 mmol/L $CaCl_2$, arrows), with a slight decrease in the perinuclear cytosolic area. C, Translocation of PKCβ-GFP from the cytosol to the plasma membrane was monitored by the plasma membrane (F_{mem}, solid line) to cytosol (F_{cyt}, dotted line) fluorescence ratio. EGTA (0.1 mmol/L), 1.2 mmol/L Ca^{2+}, 50 μmol/L ATP, and then 10 μmol/L ionomycin were added to the nominally Ca^{2+}-free medium, as indicated.

waves propagate within a very shallow subcortical area between plasma membranes and the cytosol. ATP, which is known to initiate Ca^{2+} release in the form of cytosolic Ca^{2+} waves even in the absence of extracellular Ca^{2+}, does not affect subplasmalemmal $[Ca^{2+}]$. The narrow subplasmalemmal space with small subcortical Ca^{2+} waves and the cytosol, where huge Ca^{2+} waves form, represent two distinct Ca^{2+} compartments even though they are spatially continuous.

In the resting state, a gradient between $[Ca^{2+}]_{spm}$ and extracellular $[Ca^{2+}]$ is actively maintained by continuous Ca^{2+} influx into and extrusion from the cell, seemingly resulting in no net flux of Ca^{2+} across the plasma membrane. Because the resting $[Ca^{2+}]_{spm}$ is sensitive to 2-APB (Figure 3C), the maintenance of $[Ca^{2+}]$ in the subplasmalemmal compartment may be mediated via Ca^{2+} through channels such as the IP_3 receptor, CRAC, or some of the TRP superfamily. In response to $[Ca^{2+}]_o$ elevation from 0 to 1.2 mmol/L, calibrated $[Ca^{2+}]$ increases detected by YC and NYC are $\approx$45 and 350 nmol/L, respectively, based on the method previously described.[2] Thus, vertical thickness of the subplasmalemmal compartment is estimated to be $\approx$0.2 μm, assuming the cell volume is 4500 μm^3 and the $[Ca^{2+}]_o$-sensitive compartment is absolutely confined to the subplasmalemma.

As for the bulk cytosolic Ca^{2+} waves, there are presumably mechanisms underlying the regenerative process of subcortical Ca^{2+} wave propagation because Ca^{2+} is a localized second messenger and cannot diffuse freely by itself because of the abundance of binding proteins within the cell. One candidate mediator for the formation of subcortical Ca^{2+} waves is PLC. It has been demonstrated in several cell types that a $[Ca^{2+}]_i$ increase stimulates PLC activity.[20,21] For example, voltage-gated Ca^{2+} influx through the AMPA receptor in Purkinje cells directly stimulates PLC-mediated IP_3 production, as demonstrated by the translocation of PLCδ-GFP from the plasma membrane to the cytosol.[21] PLCs are ubiquitous enzymes, and all three isozymes (β, γ, and δ) are expressed in endothelial cells.[22] Although the activities of PLCβ and PLCγ are usually regulated by G-proteins and tyrosine phosphorylation, respectively,[19,23] their catalytic properties are dependent on an optimal Ca^{2+} concentration.[22,24] Although the relative level of endothelial PLCδ activity is 7- to 8-fold lower than that of the β or γ isoenzymes,[22] its activity is more sensitive to $[Ca^{2+}]$.[25] In response to $[Ca^{2+}]$ ranging from 10^{-6} to 10^{-4} mol/L, activities of the β, γ, and δ isoenzymes of PLC, measured using PIP_2 as the substrate, were reportedly increased by approximately 50%, 200%, and 300%, respectively, with the maximal increase in activity seen at around 10^{-3} mol/L.[22] Thus, it is possible that plasmalemmal PLC in endothelial cells is also activated by Ca^{2+} influx. Activated PLC then leads to local production of IP_3,

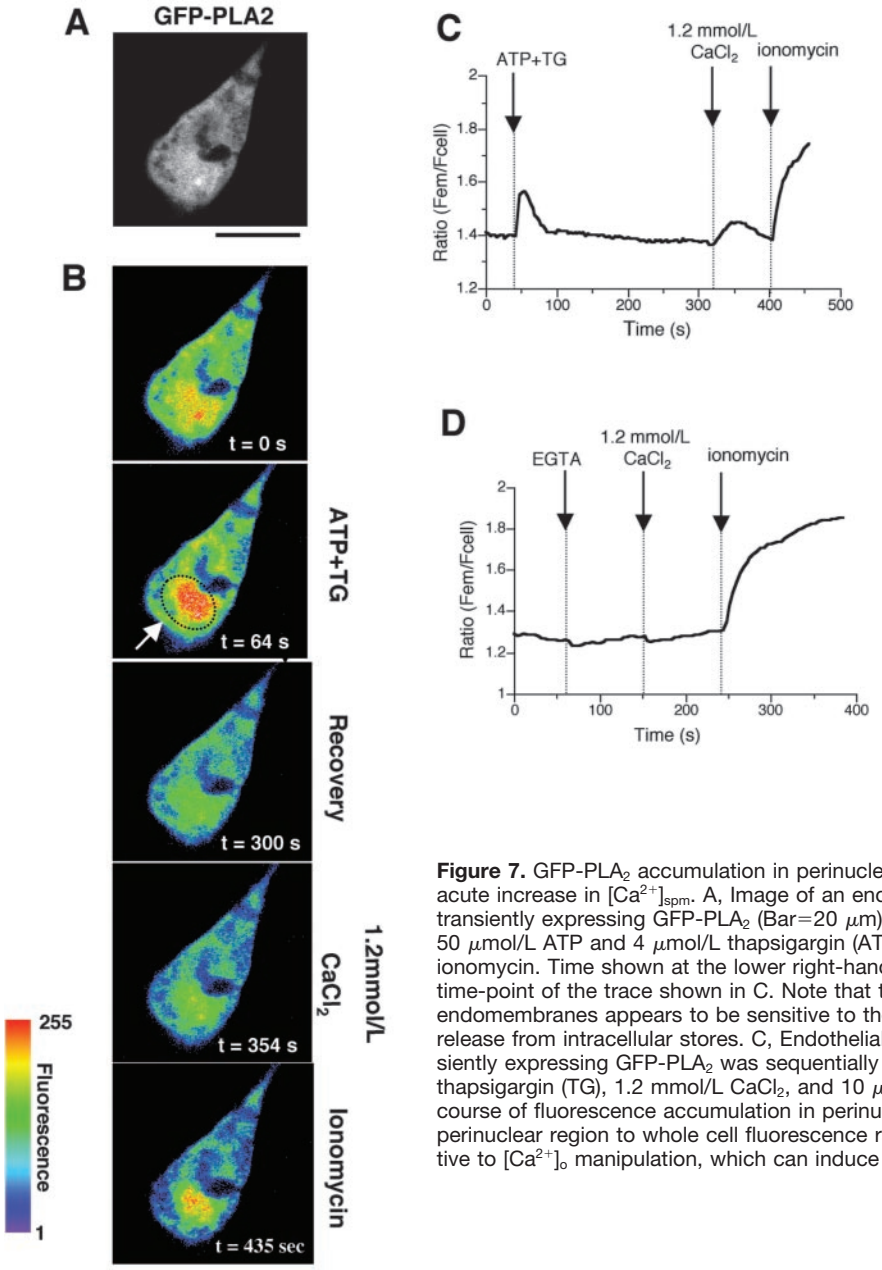

Figure 7. GFP-PLA_2 accumulation in perinuclear endomembranes is not sensitive to an acute increase in $[Ca^{2+}]_{spm}$. A, Image of an endothelial cell in nominally Ca^{2+}-free medium transiently expressing GFP-PLA_2 (Bar=20 μm). B, Cell was sequentially exposed to 50 μmol/L ATP and 4 μmol/L thapsigargin (ATP+TG), 1.2 mmol/L $CaCl_2$, and 10 μmol/L ionomycin. Time shown at the lower right-hand corner of each image corresponds to the time-point of the trace shown in C. Note that the translocation of GFP-PLA_2 to perinuclear endomembranes appears to be sensitive to the global $[Ca^{2+}]$ increase, especially Ca^{2+} release from intracellular stores. C, Endothelial cell in nominally Ca^{2+}-free medium transiently expressing GFP-PLA_2 was sequentially exposed to 50 μmol/L ATP and 4 μmol/L thapsigargin (TG), 1.2 mmol/L $CaCl_2$, and 10 μmol/L ionomycin. Trace indicates the time-course of fluorescence accumulation in perinuclear endomembranes, expressed as the perinuclear region to whole cell fluorescence ratio. D, GFP-PLA_2 accumulation is not sensitive to $[Ca^{2+}]_o$ manipulation, which can induce subcortical Ca^{2+} waves.

which might be associated with formation of the subcortical Ca^{2+} wave by IP_3-mediated Ca^{2+} influx across the plasma membrane and the sensitization of neighboring Ca^{2+} channels on the inner surface of the plasma membrane. This hypothesis is reminiscent of the widely accepted mechanisms underlying the well-characterized cytosolic Ca^{2+} waves of the IP_3-induced Ca^{2+} release from ER Ca^{2+} stores and sensitization of neighboring Ca^{2+} channels by the released Ca^{2+} itself. Ca^{2+} itself might modify the positive feedback system of regenerative Ca^{2+} propagation. For example, IP_3-induced Ca^{2+} release exhibits biphasic Ca^{2+} dependence,[26] and increased $[Ca^{2+}]_i$ directly enhances TRPC3 channels independently from the emptying of Ca^{2+} stores.[27] Our proposal is indirectly supported by the observation that subplasmalemmal IP_3 production parallels $[Ca^{2+}]_o$ changes, and that the PLC inhibitor attenuates the peak amplitude of subcortical Ca^{2+} waves. Stretch-activated Ca^{2+} channels (SAC) do not appear to play a major role in the formation of subplasmalemmal Ca^{2+} waves because Gd^{3+}, the most commonly used SAC blocker, had no effect (data not shown).

G protein–coupled PLC activation in nonexcitable cells results in IP_3 generation, which mobilizes ER Ca^{2+} stores through IP_3 receptors. This Ca^{2+} mobilization from stores is generally associated with Ca^{2+} entry, so-called store-operated or capacitative Ca^{2+} entry (CCE),[28] a process for replenishing these stores by as yet unknown mechanisms. It has been proposed that IP_3 and its receptors play essential roles not only in the release of Ca^{2+} from intracellular Ca^{2+} stores, but also in store-release–dependent Ca^{2+} entry.[1] Involvement of IP_3 in non-CCE mechanisms has also been proposed in endothelial cells[29] as well as other cell types.[30] Thus, IP_3 may directly activate Ca^{2+} entry. In fact, biochemical studies have

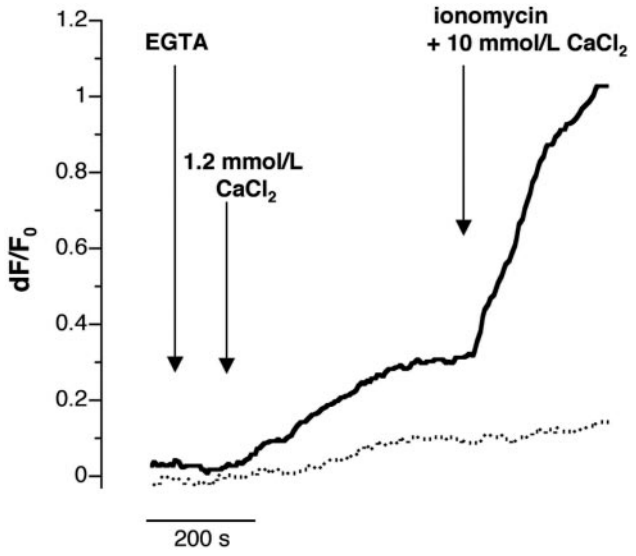

Figure 8. NO production follows the appearance of subcortical Ca^{2+} waves. Endothelial cells loaded with DAF-2 were monitored by their fluorescence in the absence (solid line) or presence (dotted line) of 10 mmol/L L-NAME. The *y*-axis denotes the ratio of fluorescence increase divided by the initial fluorescence (dF/F_0) normalized by the rate of photobleaching.

suggested the presence of IP_3R or an IP_3 receptor–like protein in the plasma membrane of many cell types,[31–34] including endothelial cells,[35] although there is little functional evidence for Ca^{2+} signaling. One exception is the documented functions of IP_3-gated Ca^{2+} channels in the olfactory neuron plasma membrane.[36] Furthermore, the propagation velocity of subcortical Ca^{2+} waves is in a range similar to that of ATP-induced Ca^{2+} waves (several tens of micrometers per second) consisting of IP_3-mediated Ca^{2+} release from intracellular Ca^{2+} stores,[37,38] suggesting a mechanistic similarity between wave propagation through the bulk cytosol and the subplasmalemma.

Correct targeting of proteins to specific subcellular sites is critical in the regulation of cellular functions. Cytoplasmic signaling proteins such as PKCβ or cytosolic PLA_2 rely on C2, one of the modular domains, for correct targeting of the plasma membrane and perinuclear membranes, respectively. PKCβ modulates thrombin-induced increases in endothelial permeability[39] or insulin-induced eNOS gene expression,[40] whereas PLA_2 catalyzes the release of arachidonic acid from phospholipids.[41] In response to an increase in the Ca^{2+} concentration, cytosolic PKCβ and PLA_2 are translocated to the membrane. This translocation is a hallmark of the activation of such molecules. Although the C2 domain of both PKCβ and PLA_2 determines their destination because of the electrostatically distinct lipid composition of phosphatidylserine-rich plasma and phosphatidylcholine-rich perinuclear membranes, respectively,[42] the two molecules could not be distinguished by differential modes of relatively large $[Ca^{2+}]$ increases: release from intracellular Ca^{2+} stores, capacitative Ca^{2+} influx, or a global nonspecific Ca^{2+} increase by ionomycin. However, only PKCβ can be recruited to the plasma membrane, with no significant PLA_2 translocation to the endomembranes, by localizing the area that is exposed to $[Ca^{2+}]$ elevation in the subplasmalemmal space. This preferential translocation of PKCβ to the plasma membrane may be attributable to the region of $[Ca^{2+}]$ elevation being the same as the targeting destination of the molecule. In response to acute changes in $[Ca^{2+}]_o$ and the resulting increase in subplasmalemmal $[Ca^{2+}]$, a small proportion of cytosolic PKCβ, which happens to be just beneath the plasma membrane binds with Ca^{2+} and is then translocated to the plasma membrane only a short distance away. Unlike PKCβ, even if a small proportion of PLA_2 binds with Ca^{2+}, it needs to travel a much longer distance to reach target perinuclear membranes. The duration of Ca^{2+} elevation is also a critical parameter for PLA_2 stabilization at the membranes.[41] In fact, depletion of extracellular Ca^{2+} does not affect the resting level of 6-keto $PGF_{1\alpha}$, a metabolite of prostacyclin produced through PLA_2 activation.[43] Thus, differential regulation of Ca^{2+}-sensitive C2-mediated translocation of cytosolic molecules can be accomplished by localizing the Ca^{2+} increase, under the plasma membrane, initiated by the formation of subcortical Ca^{2+} waves.

Effector molecules on the inner surface of the plasma membrane can also be directly affected by localized subplasmalemmal Ca^{2+} changes. Endothelial NO synthase, which is localized to the cytosolic surface of the plasmalemmal caveolae by an acylation-mediated process, is a Ca^{2+}-dependent enzyme for producing NO.[4] Endothelial cells are known to be equipped with a highly specialized and efficient Ca^{2+} delivery system for eNOS regulation. Caveolae in endothelial cells are preferential sites for capacitative Ca^{2+} entry, a mode of Ca^{2+} influx tightly linked to NO production.[2] The potent stimulating effect of Ca^{2+} influx for NO production is in contrast to that of Ca^{2+} release from internal stores, which evokes very little NO production, suggesting that the spatial factor of Ca^{2+} delivery from outside the plasma membrane is critical for efficient NO production.[2,4] As expected, eNOS activity is also sensitive to $[Ca^{2+}]_o$-dependent acute changes in $[Ca^{2+}]_{spm}$, although the amplitude of DAF-2 fluorescence is much smaller than that associated with capacitative Ca^{2+} influx or ionomycin treatment. This is consistent with previous findings that the resting level of cGMP, an indirect parameter of NO production, falls after the removal of extracellular Ca^{2+}[43]. Thus, basal eNOS activity is maintained and regulated by subplasmalemmal Ca^{2+} equilibrated with extracellular Ca^{2+}.

Finally, we have presented evidence of a novel spatially and temporally organized Ca^{2+} wave propagating through a functionally compartmentalized space beneath the plasma membrane in response to an acute increase in $[Ca^{2+}]_o$. Such acute changes in $[Ca^{2+}]_o$, although not entirely simulating actual physiological conditions, reveal functions maintained by the extracellular Ca^{2+} supply, including basal PLC activity, phospholipid metabolism, the spatiotemporal organization of subplasmalemmal Ca^{2+}, Ca^{2+}-dependent molecular translocation, and eNOS regulation. The precise mechanisms for the initiation and formation of subcortical Ca^{2+} waves require further investigation.

Acknowledgments

This work was supported by grants from the Japan Heart Foundation/ Pfizer Grant for Research on Hypertension and Vascular Metabolism,

Takeda Science Foundation, the Research Grant of the Tokyo Hypertension Conference, and the Ministry of Education, Science and Culture Grant-in-Aid for Scientific Research (15590724, 1993).

References

1. Berridge MJ, Lipp P, Bootman MD. The versatility and universality of calcium signalling. *Nat Rev Mol Cell Biol*. 2000;1:11–21.
2. Isshiki M, Yin Y, Fujita T, Anderson RGW. A molecular sensor detects signal transduction from caveolae in living cells. *J Biol Chem*. 2002;277: 43389–43398.
3. Marsault R, Murgia M, Pozzan T, Rizzuto R. Domains of high Ca^{2+} beneath the plasma membrane of living A7r5 cells. *EMBO J*. 1997;16: 1575–1581.
4. Shaul PW, Smart EJ, Robinson LJ, German Z, Yuhanna IS, Ying Y, Anderson RG, Michel T. Acylation targets endothelial nitric-oxide synthase to plasmalemmal caveolae. *J Biol Chem*. 1996;271:6518–6522.
5. Fagan KA, Smith KE, Cooper DM. Regulation of the Ca^{2+}-inhibitable adenylyl cyclase type VI by capacitative Ca^{2+} entry requires localization in cholesterol-rich domains. *J Biol Chem*. 2000;275:26530–26537.
6. Miyawaki A, Llopis J, Heim R, McCaffery JM, Adams JA, Ikura M, Tsien RY. Fluorescent indicators for Ca^{2+} based on green fluorescent proteins and calmodulin. *Nature*. 1997;388:882–887.
7. Moriyoshi K, Richards LJ, Akazawa C, O'Leary DD, Nakanishi S. Labeling neural cells using adenoviral gene transfer of membrane-targeted GFP. *Neuron*. 1996;16:255–260.
8. Skene JH, Virag I. Posttranslational membrane attachment and dynamic fatty acylation of a neuronal growth cone protein, GAP-43. *J Cell Biol*. 1989;108:613–624.
9. Zacharias D, Violin J, Newton A, Tsien RY. Partitioning of Lipid-Modified Monomeric GFPs into membrane Microdomains of Living Cells. *Science*. 2002;296:913–916.
10. Varnai P, Balla T. Visualization of phosphoinositides that bind pleckstrin homology domains: calcium- and agonist-induced dynamic changes and relationship to myo-[3H]inositol-labeled phosphoinositide pools. *J Cell Biol*. 1998;143:501–510.
11. Majlof L, Forsgren PO. Confocal microscopy: important considerations for accurate imaging. In Matsumoto B, ed. *Cell Biological Applications of Confocal Microscopy*. San Diego, Calif: Academic Press; 1993.
12. Pawley JB. *Handbook of Biological Confocal Microscopy* (*The Language of Science*). New York: Kluwer Academic Publishers; 1995:3.
13. Erickson MG, Moon DL, Yue DT. DsRed as a potential FRET partner with CFP and GFP. *Biophys J*. 2003;85:599–611.
14. Miyawaki A, Griesbeck O, Heim R, Tsien RY. Dynamic and quantitative Ca^{2+} measurements using improved cameleons. *Proc Natl Acad Sci U S A*. 1999;96:2135–2140.
15. Ma HT, Patterson RL, van Rossum DB, Birnbaumer L, Mikoshiba K, Gill DL. Requirement of the inositol trisphosphate receptor for activation of store-operated Ca^{2+} channels. *Science*. 2000;287:1647–1651.
16. Prakriya M, Lewis RS. Potentiation and inhibition of Ca^{2+} release-activated Ca^{2+} channels by 2-aminoethyldiphenyl borate (2-APB) occurs independently of IP_3 receptors. *J Physiol*. 2001;536:3–19.
17. Trebak M, Bird GS, McKay RR, Putney JW Jr. Comparison of human TRPC3 channels in receptor-activated and store-operated modes: differential sensitivity to channel blockers suggests fundamental differences in channel composition. *J Biol Chem*. 2002;277:21617–21623.
18. Hirose K, Kadowaki S, Tanabe M, Takeshima H, Iino M. Spatiotemporal dynamics of inositol 1,4,5-trisphosphate that underlies complex Ca^{2+} mobilization patterns. *Science*. 1999;284:1527–1530.
19. Rhee SG, Bae YS. Regulation of phosphoinositide-specific phospholipase C isozymes. *J Biol Chem*. 1997;272:15045–15048.
20. Kendall DA, Nahorski SR. Inositol phospholipid hydrolysis in rat cerebral cortical slices, II: calcium requirement. *J Neurochem*. 1984;42: 1388–1394.
21. Okubo Y, Kakizawa S, Hirose K, Iino M. Visualization of IP_3 dynamics reveals a novel AMPA receptor-triggered IP_3 production pathway mediated by voltage-dependent Ca^{2+} influx in Purkinje cells. *Neuron*. 2001;32:113–122.
22. Fu Y, Cheng JX, Hong SL. Characterization of cytosolic phospholipases C from porcine aortic endothelial cells. *Thromb Res*. 1994;73:405–417.
23. Rebecchi MJ, Pentyala SN. Structure, function, and control of phosphoinositide-specific phospholipase C. *Physiol Rev*. 2000;80:1291–1335.
24. Akhtar RA, Abdel-Latif AA. Carbachol causes rapid phosphodiesteratic cleavage of phosphatidylinositol 4,5-bisphosphate and accumulation of inositol phosphates in rabbit iris smooth muscle; prazosin inhibits noradrenaline- and ionophore A23187-stimulated accumulation of inositol phosphates. *Biochem J*. 1984;224:291–300.
25. Allen V, Swigart P, Cheung R, Cockcroft S, Katan M. Regulation of inositol lipid-specific phospholipase cΔ by changes in Ca^{2+} ion concentrations. *Biochem J*. 1997;327:545–552.
26. Iino M. Biphasic Ca^{2+} dependence of inositol 1,4,5-trisphosphate-induced Ca^{2+} release in smooth muscle cells of the guinea pig taenia caeci. *J Gen Physiol*. 1990;95:1103–1122.
27. Ohki G, Miyoshi T, Murata M, Ishibashi K, Imai M, Suzuki M. A calcium-activated cation current by an alternatively spliced form of Trp3 in the heart. *J Biol Chem*. 2000;275:39055–39060.
28. Putney JW Jr. Capacitative calcium entry revisited. *Cell Calcium*. 1990; 11:611–624.
29. Vaca L, Kunze DL. IP_3-activated Ca^{2+} channels in the plasma membrane of cultured vascular endothelial cells. *Am J Physiol*. 1995;269: C733–C738.
30. Kuno M, Gardner P. Ion channels activated by inositol 1,4,5-trisphosphate in plasma membrane of human T-lymphocytes. *Nature*. 1987;326:301–304.
31. Khan AA, Steiner JP, Klein MG, Schneider MF, Snyder SH. IP_3 receptor: localization to plasma membrane of T cells and cocapping with the T cell receptor. *Science*. 1992;257:815–818.
32. Khan AA, Steiner JP, Snyder SH. Plasma membrane inositol 1,4,5-trisphosphate receptor of lymphocytes: selective enrichment in sialic acid and unique binding specificity. *Proc Natl Acad Sci U S A*. 1992;89: 2849–2853.
33. Feng L, Kraus-Friedmann N. Association of the hepatic IP_3 receptor with the plasma membrane: relevance to mode of action. *Am J Physiol*. 1993;265:C1588–C1596.
34. Mayrleitner M, Schafer R, Fleischer S. IP_3 receptor purified from liver plasma membrane is an $(1,4,5)IP_3$ activated and $(1,3,4,5)IP_4$ inhibited calcium permeable ion channel. *Cell Calcium*. 1995;17:141–153.
35. Fujimoto T, Nakade S, Miyawaki A, Mikoshiba K, Ogawa K. Localization of inositol 1,4,5-trisphosphate receptor-like protein in plasmalemmal caveolae. *J Cell Biol*. 1992;119:1507–1513.
36. Okada Y, Teeter JH, Restrepo D. Inositol 1,4,5-trisphosphate-gated conductance in isolated rat olfactory neurons. *J Neurophysiol*. 1994;71: 595–602.
37. Isshiki M, Ando J, Korenaga R, Kogo H, Fujimoto T, Fujita T, Kamiya A. Endothelial Ca^{2+} waves preferentially originate at specific loci in caveolin-rich cell edges. *Proc Natl Acad Sci U S A*. 1998;95:5009–5014.
38. Jaffe LF, Creton R. On the conservation of calcium wave speeds. *Cell Calcium*. 1998;24:1–8.
39. Vuong PT, Malik AB, Nagpala PG, Lum H. Protein kinase C beta modulates thrombin-induced Ca^{2+} signaling and endothelial permeability increase. *J Cell Physiol*. 1998;175:379–387.
40. Kuboki K, Jiang ZY, Takahara N, Ha SW, Igarashi M, Yamauchi T, Feener EP, Herbert TP, Rhodes CJ, King GL. Regulation of endothelial constitutive nitric oxide synthase gene expression in endothelial cells and in vivo: a specific vascular action of insulin. *Circulation*. 2000;101: 676–681.
41. Hirabayashi T, Kume K, Hirose K, Yokomizo T, Iino M, Itoh H, Shimizu T. Critical duration of intracellular Ca^{2+} response required for continuous translocation and activation of cytosolic phospholipase A_2. *J Biol Chem*. 1999;274:5163–5169.
42. Stahelin RV, Rafter JD, Das S, Cho W. The molecular basis of differential subcellular localization of C2 domains of protein kinase C-alpha and group IVa cytosolic phospholipase A_2. *J Biol Chem*. 2003;278: 12452–12460.
43. White DG, Martin W. Differential control and calcium-dependence of production of endothelium-derived relaxing factor and prostacyclin by pig aortic endothelial cells. *Br J Pharmacol*. 1989;97:683–690.

Circulation Research
JOURNAL OF THE AMERICAN HEART ASSOCIATION

Subcortical Ca^{2+} Waves Sneaking Under the Plasma Membrane in Endothelial Cells

Masashi Isshiki, Akiko Mutoh and Toshiro Fujita

Circ Res. 2004;95:e11-e21; originally published online July 8, 2004;
doi: 10.1161/01.RES.0000138447.81133.98
Circulation Research is published by the American Heart Association, 7272 Greenville Avenue, Dallas, TX 75231

Print ISSN: 0009-7330. Online ISSN: 1524-4571